

Specific Heat of Liquid He³/He⁴ Mixtures near the Junction of the λ and Phase-Separation Curves. I*

T. A. Alvesalo, P. M. Berglund, S. T. Islander, and G. R. Pickett†

Department of Technical Physics, Technical University of Helsinki, Otaniemi, Finland

and

W. Zimmermann, Jr.

School of Physics and Astronomy, University of Minnesota, Minneapolis, Minnesota 55455

(Received 16 July 1971)

The specific heat of liquid He³/He⁴ mixtures has been measured at saturated vapor pressure for eight values of the He³ mole fraction x in the range $0.53 \leq x \leq 0.73$ at temperatures from ~ 0.6 to ~ 1.4 °K. For purposes of comparison, the specific heat of pure liquid He³ has also been measured under similar conditions. The measured specific heat, obtained with a calorimeter almost completely full of liquid, has been corrected to yield the specific heat of the liquid $c_{P,x}$ at constant pressure and mole fraction. For the mixtures, the correction required was everywhere $\lesssim 1\%$. To a resolution in temperature which varies from 0.1 to 3 m°K from one value of x to another, the specific heat at the λ peak appears to be finite, continuous, and cusped. Both the λ peak and the discontinuity in $c_{P,x}$ as the system goes from the two-liquid-phase region to the one-liquid-phase region tend to disappear as the junction of phase boundaries is approached.

I. INTRODUCTION

The natures of the λ transition in liquid He³/He⁴ mixtures and of the junction of the λ and phase-separation curves have recently become topics of considerable interest.¹ Of particular interest is the question of how the critical behavior of the mixtures at the λ curve changes as the relative concentration of He³ in the mixture increases from 0 to the value at the junction. Also of great interest are the unique properties of the junction itself.

Our interest in the mixtures was stimulated by the phase-boundary results of Graf, Lee, and Reppy which were obtained from dielectric-constant and thermal-conduction measurements on the mixtures near the junction.² These results indicated that in the T, x plane at saturated vapor pressure the λ curve and the two arms of the phase-separation curve all meet with finite nonzero slopes at a junction point $T_0 \cong 0.87$ °K, $x_0 \cong 0.67$ which lies at the top of the phase-separation region. Here T is the absolute temperature, and x is the He³ mole fraction of the mixture defined as the ratio $N_3/(N_3 + N_4)$, where N_3 and N_4 are respectively the numbers of moles of He³ and He⁴ in the sample. As Rice has pointed out, the λ and phase-separation transitions in the mixtures seem to be intimately related, and the situation is one in which a second-order transition goes over into a first-order transition with decreasing temperature.³

The present measurements at saturated vapor pressure of the molar specific heat of the liquid $c_{P,x}$ at constant pressure and mole fraction were undertaken to explore further the thermodynamic behavior of the mixtures near the junction, with

greater resolution than had been obtained in the earlier specific-heat measurements of de Bruyn Ouboter, Taconis, le Pair, and Beenakker.⁴ A preliminary account of our work has appeared.⁵

Several other experimental investigations on the liquid mixtures having a close relation to our work have recently been carried out. Gasparini and Moldover have reported the results of high-resolution measurements of $c_{P,x}$ near the λ curve for values of x in the range $0 \leq x \leq 0.40$.⁶ Measurements near the λ curve of the specific heat $c_{v,x}$ at constant molar volume v and mole fraction $x=0.09$ have been reported by Tang, Zipfel, and Graf.⁷ High-resolution vapor-pressure measurements, which provide thermodynamic information about the liquid complementary to that given by the specific heat, have been carried out by Goellner and Meyer.⁸ In addition, attention has recently been called to the unique nonclassical nature of the junction in a theoretical paper by Griffiths.⁹

The present report describes the experiment and gives the results of specific-heat measurements carried out at eight values of x in the range $0.53 \leq x \leq 0.73$. As a check upon our experimental technique, measurements of the molar specific heat of pure He³ at saturated vapor pressure were also made, and the results are included in this report. The temperature range covered was approximately 0.6 to 1.4°K. Some earlier measurements on the mixtures were made at additional values of x ,⁵ but because of subsequent improvements in apparatus and technique they have not been included in the present paper. The report concludes with a preliminary analysis and discussion of the data. It is intended to present further

INNER PARTS OF THE CRYOSTAT

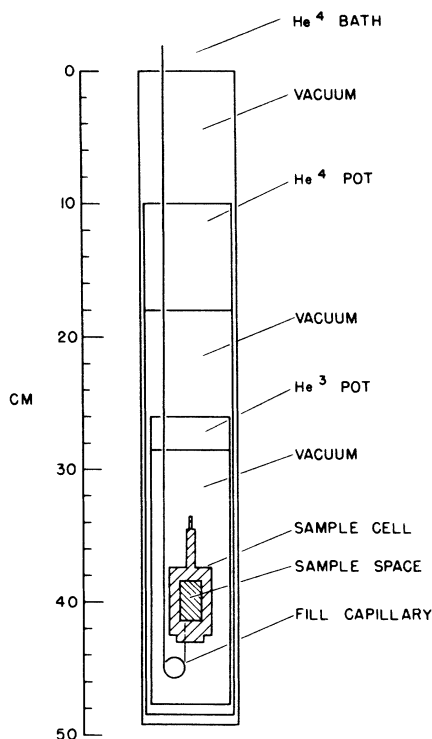


FIG. 1. Diagram of the inner parts of the cryostat.

analysis of the results in a later paper.

II. THERMODYNAMIC FRAMEWORK

In treating the mixtures thermodynamically one may take as a starting point the differential relation

$$dG = -S dT + V dP + \mu_3 dN_3 + \mu_4 dN_4, \quad (1)$$

in which G is the total Gibbs free energy of the system, S is the entropy, V is the volume, and μ_3 and μ_4 are the respective molar chemical potentials of the He³ and He⁴ components. Reducing the extensive quantities in this expression to intensive quantities per mole of mixture, denoted by lower case letters, one obtains the useful relation

$$dg = -s dT + v dP + \phi dx, \quad (2)$$

where $\phi = \mu_3 - \mu_4$. Thus ϕ appears as the natural thermodynamic variable conjugate to x .

It is helpful to note that when P is constant, and thus dP zero, Eq. (2) for the mixtures is analogous to the relation for a pure fluid

$$df = -s dT - P dv, \quad (3)$$

where f is the molar Helmholtz free energy. In this analogy f corresponds to g , P to $-\phi$, and v

to x . Hence in studying the mixtures at constant P , which is very nearly the case at saturated vapor pressure, one may borrow freely from formalism developed for pure fluids.

Since T , P , and x are convenient independent variables from an experimental point of view, we shall make extensive use of Eq. (2). Sometimes, however, it is more convenient to regard the three "fields" T , P , and ϕ as independent variables.^{9,10} In this case one may make a Legendre transformation to a new potential $g - \phi x$, which turns out to be $\mu_4(T, P, \phi)$, obtaining the alternative fundamental differential relation

$$d\mu_4 = -s dT + v dP - x d\phi. \quad (4)$$

A word about notation: We will denote the λ curve (surface) by the symbol λ and the phase-separation curve (surface) by σ . When it is necessary to distinguish the He³-rich and He³-poor sides of the λ curve or the corresponding branches of the phase-separation curve we will use the symbols $+$ and $-$, respectively. When a derivative is to be taken at constant pressure a subscript P will be used. When no such subscript appears, the derivative is to be taken at saturated vapor pressure unless the context dictates otherwise. Thus, for example, a derivative denoted $()_{P,\lambda}$ is to be evaluated along the intersection of a surface of constant pressure with the λ surface, while a derivative denoted simply $()_\lambda$ is to be evaluated along the intersection of the saturated vapor pressure surface with the λ surface, i. e., along the usual λ curve.

III. APPARATUS AND PROCEDURE

A. Description of Cryostat

The measurements were made in a cryostat of conventional design employing unpumped liquid N₂ and He⁴ outer baths and pumped inner He⁴ and He³ baths. The arrangement of the inner parts of the cryostat is shown in Fig. 1. The sample cell consisted of a cylinder of high-purity copper with a cylindrical cavity 1.6 cm in diameter and 3.0 cm high, into which a tangled mass of 0.007-cm-diameter high-purity bare copper wire had been compressed to ensure good thermal contact between sample and cell. The copper wire occupied approximately 55% of the cavity volume, leaving an open space of 2.85 cm³ for the sample. This open volume was determined to within $\pm 1.0\%$ by measuring, at two different values of x , the amount of liquid He³/He⁴ mixture needed to overfill the cell at a fixed temperature near 1.0°K. Use was made here of the measurements of the molar volume of the liquid mixtures by Kerr.¹¹ The total mass of the copper used in the construction of the sample cell was approximately 310 g.

A bifilar heater of approximately 500- Ω resis-

tance was wound in an open helix around the sides of the cell and varnished in place. Two germanium resistance thermometers, which we designate *A* and *B*,¹² were placed in holes drilled into the upper part of the cell, and care was taken to provide good thermal contact between both the container and the leads of each thermometer and the cell. Four-wire electrical connections to each of the thermometers from a terminal post thermally anchored to the He³ pot were made using 0.008-cm-diameter manganin wires approximately 10 cm long. Superconducting connections to the heater were made with two indium-coated manganin wires of the same dimensions. Four-wire heater connections were then used between the He³ pot and the heater current supply.

The sample cell was firmly supported below the He³ pot by means of spring-loaded nylon threads. The cell was cooled by means of a mechanical jaw-type heat switch and was never exposed to exchange gas in the course of a run before or during specific-heat measurements. The support of the sample cell and the arrangement of the heat switch were very similar to those shown by Hill and Pickett.¹³

The experiment was planned so that the sample would nearly but never entirely fill the cell with liquid, the vapor space assuring that the sample would remain at saturated vapor pressure. The sample was admitted to the cell through a long capillary running from a valve at the top of the cryostat down through the main He⁴ bath into the vacuum can. The capillary passed through the He⁴ and He³ pots, to which it was thermally anchored, and finally entered the cell at the bottom, so that a portion of the capillary would always be filled with liquid, whose thermal conduction was known to be low even in the superfluid region.¹⁴ The upper section of capillary running from the valve to the flange at the top of the vacuum can had an inner diameter of ~ 0.065 cm and a length of ~ 95 cm, the inner volume thus amounting to 0.3 cm³. The volume of the additional dead space on the lower side of the valve at room temperature was of the order of 1 cm³. The lower section of the capillary extending from the flange to the cell, the only section which liquid could have occupied, consisted of a cupronickel tube of 67-cm length and 0.025-cm inner diameter partially filled along a section of its length by a 0.020-cm-diameter stainless-steel wire. The total volume of the empty space remaining in this tube was 0.018 ± 0.006 cm³.

The principal advantage of a direct capillary connection between the cell and the top of the cryostat was the avoidance of any difficulties that might have been associated with the use of a low-temperature valve. At the values of x studied the heat leak between the cell and He³ pot due to liquid in the capillary is estimated to have been much less

than 1 erg/sec.

The main disadvantage of this arrangement was that a certain fraction of the sample lay outside the sample cell, an amount which must have increased with temperature as the increase in the vapor pressure within the cell tended to push more of the liquid out into the fill capillary. However, it is estimated that the total fraction of the sample lying outside of the cell remained between the limits of 0.3 and 0.9%, and we believe that our estimates of the amount of sample in the cell at any given temperature relative to the total amount of sample present are accurate to within an uncertainty of $\pm 0.3\%$.

Another, related disadvantage was that, due to temperature gradients and heat currents in the capillary, fractionation of the mixture in the capillary may have taken place, tending to alter the value of x within the cell. However, under extreme assumptions it is unlikely that x within the cell was altered by more than ± 0.003 , and under usual conditions the alteration should have been much less.

In retrospect, it seems possible that had the capillary entered the top of the cell these disadvantages might have been avoided without seriously increasing the heat leak to the cell. At the time of the design of the apparatus it was feared that in the superfluid region, film flow and vapor reflux might cause a large heat leak along a vapor-filled capillary. However, because in the mixtures the He³ atoms do not participate in the film flow, the reflux of He⁴ atoms would be impeded by a stationary distribution of He³ atoms in the vapor, and it seems likely that the process would have contributed a much smaller heat leak than in the case of pure He⁴.

B. Cell Heating and Thermometry

Direct current was supplied to the sample-cell heater from a constant-current source. Currents in the range from 0.1 to 0.3 mA were used for most of the work, there being an indication on some occasions that larger currents gave rise to inconsistent data. It is estimated that the energies in the heat pulses delivered to the sample cell were determined with an over-all uncertainty of $\pm 0.6\%$.

The resistance of thermometer *A*, the thermometer used for the bulk of the measurements, was measured potentiometrically using direct current. A measuring current of ~ 4.5 μ A was employed, corresponding to a power of ~ 2 nW dissipated in the thermometer at 1.0° K, where its resistance was ~ 120 Ω . Because the sensitivity of this thermometer $d \ln R / d \ln T$ was ~ -1.7 at 1.0° K and the minimum detectable voltage change with our system was ~ 10 nV, the minimum detectable temperature change at this temperature was ~ 10 μ °K. Because the power being dissipated in this thermometer was large enough to cause a significant shift in the re-

sistance from the zero-power limit, care was always taken to use the same value of measuring current, which was derived from a stable high-impedance source.

Thermometer *A* was calibrated between 0.5 and 1.7 °K against the 1962 He³ vapor-pressure scale of temperature¹⁵ to an estimated accuracy of $\sim \pm 1$ m°K above 0.6 °K. The He³ in the He³ pot used in the calibration was purified of He⁴ to less than ~ 5 parts in 10⁴ by fractional distillation,¹⁶ and the vapor-pressure scale was then used without correction for the He⁴ present, the resulting error being < 0.2 m°K.¹⁷ No correction was made for thermomolecular pressure drop, the estimated correction at 0.6 °K being < 0.3 m°K and decreasing rapidly with increasing temperature.¹⁸ The error in specific heat resulting from neglect of such thermomolecular effects is estimated to be $< 1\%$ at 0.6 °K and $< 0.1\%$ at 0.7 °K. The calibration of the thermometer was rechecked a number of times during the course of the work, after many thermal cycles back to room temperature, and there was no convincing evidence of any shifts of more than a few tenths of a millidegree having taken place. It is estimated that except possibly at the lowest temperatures the uncertainty in specific heat resulting from systematic errors in calibration was $< 0.5\%$.

Thermometer *B* was used only for the higher-resolution data taken for $x = 0.530, 0.650,$ and 0.680 . Its resistance was measured using an ac ratio-transformer bridge. This bridge was designed so that lead resistances were balanced to first order and that any higher-order effects could easily be measured potentiometrically and corrected for. A measuring voltage of ~ 40 mV rms applied to this thermometer at 1.0 °K, where its resistance was ~ 27 k Ω , corresponded to a power dissipation of ~ 60 nW in the thermometer. Because the sensitivity of this thermometer $d \ln R / d \ln T$ was ~ -3.7 at 1.0 °K and the minimum detectable voltage change was ~ 20 nV, the minimum detectable temperature change with this thermometer at this temperature was $\sim 0.3 \mu^\circ\text{K}$.

Thermometer *B* was calibrated against thermometer *A*, a process which could easily be repeated from day to day during a run. Drifts in the calibration of thermometer *B* relative to thermometer *A* may have been due to the power sensitivity of thermometer *B* in connection with drifts in the excitation voltage, since rather high power levels were used.

C. Sample Preparation

Samples of known composition were prepared near room temperature by mixing pure He⁴ gas with relatively pure He³ gas whose He⁴ impurity concentration was known. The resulting mole fraction x of He³ in the sample was determined by in-

roducing first one gas then the other into a fixed volume at a constant temperature of 0 °C while measuring the pressures with a quartz bourdon-tube manometer.¹⁹ At mixing pressures of less than 1 atm, corrections due to the nonideality of the gas were unnecessary for our purposes.²⁰ Care was taken to trap out any air and other more condensable gases in the He³ and He⁴ previous to mixing. It is estimated that the x values of mixtures prepared in this way were determined to within ± 0.001 . For the measurements on pure He³, He³ gas containing less than 1 part He⁴ in 10³ was used.

For the measurements of specific heat, a known quantity of gas was condensed into the cryostat with the cell held at some conveniently low temperature near 1 °K. The amount of gas introduced into the cryostat was determined by measuring the initial and final pressures of the mixture in a measured volume of the system from which the gas was condensed. This amount was rechecked in several cases at the end of the run when the sample was recovered from the cryostat. The quantity of sample was typically ~ 0.08 mole and was believed to be known to within an uncertainty of $\pm 0.3\%$.

Several precautions were taken to minimize any fractionation effects which would yield a sample in the cryostat whose composition was different from that of the original gas mixture. First, the amount of gas mixture prepared for a given sample was only about 10% greater than the amount to be condensed into the cryostat. Next, the condensation was carried out as steadily and quickly as possible, the time required being typically 2 h. Finally, once the sample had been introduced, the sample valve at the top of the cryostat was closed and left so during the run, no withdrawals of sample taking place until the entire sample was removed. No attempts were made to prepare mixtures or change the composition at low temperature; all the mixing was carried out at 0 °C.

D. Measurement of Specific Heat

Measurements of the total heat capacity were made by the conventional method of following the temperature drift of the cell before heating, adding a known amount of heat ΔQ , and then once again following the temperature drift. The effective initial and final temperatures of the measurement were determined by extrapolating the initial and final drift curves to the center of the heating interval, and the average total heat capacity in this effective temperature interval ΔT was determined by dividing ΔQ by ΔT . This simple extrapolation procedure was justified by the slowness of the drift and the absence of any abrupt changes in it, and by the relatively small changes taking place in the heat capacity within the temperature intervals used. Typically, the drift intervals between heating

periods were ~ 900 sec long, the drift rate near the features of interest was within the range $\pm 0.5 \mu^\circ\text{K sec}^{-1}$, depending upon the temperatures of the cell and He^3 pot, the heating periods were from 20 to 600 sec long, and the temperature rise during heating was from 0.1 to $40 \text{ m}^\circ\text{K}$.

For many samples two series of points were taken covering the entire temperature range from ~ 0.6 to $\sim 1.4 \text{ }^\circ\text{K}$ with relatively large heat pulses, corresponding to temperature intervals of 30 to $40 \text{ m}^\circ\text{K}$ or more. In between these series, higher-resolution measurements were made in the vicinity of the phase boundaries. Because the features of the specific heat that are of interest in this work appear on top of a relatively large background specific heat, it seemed desirable to achieve a relative accuracy in specific heat of a few tenths of a percent. As a result the smallest heating interval we could use with thermometer *A*, with a resolution of $\sim 10 \mu^\circ\text{K}$, was $\sim 3 \text{ m}^\circ\text{K}$; the smallest with *B*, with a resolution of $\sim 0.3 \mu^\circ\text{K}$, was $\sim 0.1 \text{ m}^\circ\text{K}$. These smallest intervals thus represent the effective temperature resolution of our specific-heat measurements.

Immediately following the heating period, the temperature drift curve showed a rapid relaxation toward a steady drift with a time constant of a few seconds. This primary relaxation did not vary greatly over the entire range of temperature and composition covered, and it seems likely that it represented the primary thermal relaxation between the cell and its contents. In addition to this primary relaxation there was some indication that additional relaxation of smaller magnitude was taking place on a time scale of hundreds of seconds, probably associated with redistribution of the two helium isotopes among the various phases of the two- or three-phase system. Although drift periods of ~ 900 sec appeared to be long enough to prevent interference from this secondary relaxation, there is of course no guarantee that steady-state drift was actually attained and that longer relaxation times were not present. Long-term relaxation effects were particularly noticeable in the three-phase region at temperatures immediately below the phase-separation boundary for $x \lesssim x_0$, and the tendency of the data to scatter there rather more than in other regions suggests that the drift periods were not always long enough to achieve steady state. The effect of using too short a drift period was to yield spuriously low values of specific heat which were drift period dependent. In retrospect, it would have been advantageous to use a cell cavity with a much smaller height, so as to reduce the relaxation time associated with isotopic redistribution.

The average specific heat c per mole of sample was computed from the total heat capacity by sub-

tracting away the relatively small heat capacity of the empty cell and then dividing by the total number of moles of sample present in the cell. The heat capacity of the empty cell amounted to $\lesssim 1\%$ of the total heat capacity. This cell heat capacity was measured directly and was accounted for almost entirely by the copper used in the cell's construction.

Taking into account the precision with which the various measurements were made, it is estimated that c was determined to within an over-all absolute uncertainty of $\pm 1.8\%$ over most of the temperature range. The relative uncertainty between many of the determinations of c was considerably less than this.

IV. RESULTS

Because the cell was only partially full of liquid during measurement of the specific heat, the over-all molar specific heat c of the sample was not that of the liquid alone but contained contributions due to the vapor in the cell and to evaporation of the liquid with increase of temperature. As a consequence c depended on the amount of sample present. In the interest of presenting the results in a useful form, it was decided to compute from c the molar specific heat $c_{P,x}$ of the liquid alone at constant pressure and He^3 mole fraction, evaluated at saturated vapor pressure. In the case that two liquid phases are present, as in the phase-separation region, $c_{P,x}$ denotes the average molar specific heat of the liquid phases at constant pressure and average He^3 mole fraction of the liquid.

It can be shown thermodynamically that for a sample consisting of N_3 moles of He^3 and N_4 moles of He^4 contained in a cell of fixed volume V , the over-all molar specific heat c of the sample may be written

$$c = -T \left(x \frac{d^2\mu_3}{dT^2} + (1-x) \frac{d^2\mu_4}{dT^2} \right) + \frac{VT}{N} \frac{d^2P}{dT^2}, \quad (5)$$

when one, two, or three phases are present.²¹ Here $x = N_3/(N_3 + N_4)$ is the average mole fraction of He^3 in the sample, and $N = N_3 + N_4$ is the total number of moles present. The derivatives apply to the thermodynamic path actually followed by the system. When three phases are present in equilibrium, the path is uniquely determined by the co-existence conditions, and consequently the derivatives are unique functions of T . When only one or two phases are present, these derivatives depend not only on T but also on x and on the average molar volume $v = V/N$ of the sample.

From Eq. (5) can be derived the expression

$$c = \sum_i \frac{N_i}{N} \left[c_{P,x} - 2T \left(\frac{\partial v}{\partial T} \right)_{P,x} \frac{dP}{dT} - T \left(\frac{\partial v}{\partial P} \right)_{T,x} \left(\frac{dP}{dT} \right)^2 \right]$$

$$+ T \left(\frac{\partial \phi}{\partial x} \right)_{P,T} \left(\frac{dx}{dT} \right)^2 \Big]_i, \quad (6)$$

where i runs over whatever phases are present, N_i is the number of moles of the i th phase present, and for the i th phase x is the He³ mole fraction, v is the molar volume, and $c_{P,x}$ is the molar specific heat at constant P and x . The total derivatives dP/dT and dx/dT in this expression apply to the paths in P, T, x space actually followed by the individual phases present. A derivation of this expression is given in the Appendix.

When the amount of sample within the cell is not fixed but can vary, such as it did in our experiment as material in one of the phases left the cell with increasing temperature, Eqs. (5) and (6) must be modified by the addition of the term $-(Tv/N)(dP/dT) \times (dN/dT)$ to the right-hand sides. Here v is the molar volume of the phase leaving the cell, in our case a liquid phase. However, we estimate that with one exception this term made a negligible contribution to our results, and so we have not included this term in computing $c_{P,x}$ for the liquid from c . The only exception is mentioned later on in the discussion of the results for pure He³.

The first step in obtaining $c_{P,x}$ for the liquid from c was to evaluate and subtract away the vapor term in the expression for c given by Eq. (6). Under our experimental conditions, in which (with the exception of run 3 with pure He³) the cell volume was always between 93 and 97% full of liquid, N_v/N was always very small. Here N_v is the number of moles of vapor present. As a consequence the vapor-phase term in Eq. (6) was relatively small and could be estimated to sufficient accuracy using ideal-gas approximations for $c_{P,x}$ and the partial derivatives, as well as for N_v . In these calculations use was made of the vapor-pressure data of Sydoriak and Roberts²² in combination with the He³ vapor pressures of the T_{62} scale,¹⁵ the determinations of $x_v(x_l, T)$ by Roberts and Swartz²³ and an approximate form for $x_v(x_l, T)$ based on regular solution theory,²⁴ and the liquid molar volume results of Kerr.¹¹ A further consequence of the smallness of N_v/N was that the average mole fraction of the liquid x_l never differed from x by more than -0.0004 due to the presence of vapor in the cell.

The vapor-phase term was subtracted from c and the result multiplied by N/N_l to yield the quantity c' given by the expression

$$c' = \sum_i \frac{N_i}{N_l} \left[c_{P,x} - 2T \left(\frac{\partial v}{\partial T} \right)_{P,x} \frac{dP}{dT} - T \left(\frac{\partial v}{\partial P} \right)_{T,x} \left(\frac{dP}{dT} \right)^2 + T \left(\frac{\partial \phi}{\partial x} \right)_{P,T} \left(\frac{dx}{dT} \right)^2 \right]_i, \quad (7)$$

where i now designates just the one or two liquid phases present and $N_l = N - N_v$ is the number of

moles of liquid in the cell. This specific heat c' has the physical significance of being the molar specific heat that one would measure in the limit of the cell being (not quite) completely filled with liquid.

The greatest uncertainty in the calculation of c' from c occurs near the λ transition, where dP/dT changes rapidly with temperature. However, due to the smallness of the vapor term relative to the liquid term, the uncertainty in c' due to this source is still quite small. The net negative correction to c yielding c' increased in magnitude with T and with the exception of run 3 with pure He³ was never greater in magnitude than $0.09 \text{ J mole}^{-1} \text{ }^\circ\text{K}^{-1}$; at T_λ it was never greater in magnitude than $0.04 \text{ J mole}^{-1} \text{ }^\circ\text{K}^{-1}$, and its uncertainty there due to the uncertainty in dP/dT was always well within $\pm 0.01 \text{ J mole}^{-1} \text{ }^\circ\text{K}^{-1}$.

The last step in determining $c_{P,x}$ for the liquid from c was to extract $c_{P,x}$ from c' . In the two-liquid-phase region, the contributions to c' due to the terms proportional to dP/dT and $(dP/dT)^2$ were estimated to be everywhere much less in magnitude than $0.01 \text{ J mole}^{-1} \text{ }^\circ\text{K}^{-1}$ and hence negligible. These estimates involved use not only of the vapor-pressure data of Sydoriak and Roberts for dP/dT ,²² but also of the molar volume measurements of Kerr for $(\partial v/\partial T)_{P,x}$,¹¹ and of the speed of sound measurements of Roberts and Sydoriak for $(\partial v/\partial P)_{T,x}$.²⁵ Further, the difference between $(dx/dT)_\sigma$ for each liquid phase in equilibrium with the other and the vapor and $(dx/dT)_{P,\sigma}$ for each liquid phase in equilibrium with the other at constant pressure was estimated to have been negligibly small for our purposes. Thus in the two-liquid-phase region c' represents without further correction the average molar specific heat $c_{P,x}$ of the liquid as a whole at constant pressure P and average mole fraction x_l , which can be written

$$c_{P,x} = \frac{x_+ - x_-}{x_+ - x_-} \left[c_{P,x} + T \left(\frac{\partial \phi}{\partial x} \right)_{P,T} \left(\frac{dx}{dT} \right)^2 \right]_{-} + \frac{x_l - x_-}{x_+ - x_-} \left[c_{P,x} + T \left(\frac{\partial \phi}{\partial x} \right)_{P,T} \left(\frac{dx}{dT} \right)^2 \right]_{+}, \quad (8)$$

where $+$ and $-$ refer respectively to the He³-rich and He³-poor liquid phases in equilibrium.

In the one-liquid-phase region, the sum in Eq. (7) contains only one member. In order to obtain $c_{P,x}$ for the liquid from c' in this region the terms in Eq. (7) proportional to dP/dT and $(dP/dT)^2$ were estimated using the data cited above. Special care was required near T_λ where not only rapid changes in dP/dT with T occur but also the possibility exists that the derivatives $(\partial v/\partial T)_{P,x}$ and $(\partial v/\partial P)_{T,x}$ become large in magnitude. However, at values of x near x_0 the molar-volume and sound-velocity data from which these derivatives were estimated show no

anomaly. Further, the extreme values attained by these derivatives may be estimated from the measured specific heat and estimates of other thermodynamic functions using relations implicit in the work of Buckingham and Fairbank on pure He⁴.²⁶ Such estimates indicate that for our purposes any anomaly in these derivatives at T_λ is negligible. The term in Eq. (7) proportional to $(dx/dT)^2$ for the liquid was estimated in the one-liquid-phase region to be everywhere considerably less than 0.001 J mole⁻¹ °K⁻¹ under our conditions and thus completely negligible. Like the magnitude of the correction to c yielding c' , the magnitude of the overall positive correction to c' yielding $c_{P,x}$ reached its largest values at the highest temperatures. Except for pure He³, it was never greater than 0.06 J mole⁻¹ °K⁻¹ and at T_λ was always $\ll 0.01$ J mole⁻¹ °K⁻¹. The two corrections tended to cancel each other at the high-temperature end of the range, so that except for pure He³ the magnitude of the total correction to c yielding $c_{P,x}$ never exceeded 0.06 J mole⁻¹ °K⁻¹ ($\leq 1\%$ of $c_{P,x}$). For pure He³ the total correction remained < 0.10 J mole⁻¹ °K⁻¹ in magnitude.

The data, corrected point by point to yield $c_{P,x}$ for the eight mixtures measured, were tabulated along with the average temperatures of the measurements.²⁷ Selective plots of these data for five representative mixtures are shown in Fig. 2. Not all of the data points tabulated for these mixtures have been included in the plots. In particular, points whose initial and final temperatures clearly spanned either the phase-separation temperature T_σ or the λ temperature T_λ have not been plotted; nor have two series of points for $x < x_0$ measured near T_σ which are suspected to lie spuriously low for $T < T_\sigma$ been plotted. Values of T_σ and T_λ estimated from these data by inspection of plots such as those of Fig. 2 are listed in Table I and are plotted as solid circles in Fig. 3. We estimate from a plot of this type that the junction lies at T_0

TABLE I. Various parameters for the eight mixtures studied and for pure He³. Here $N(\text{total})$ represents the total number of moles in the sample.

x	$N(\text{total})$ (moles)	T_σ (°K)	T_λ (°K)
0.530 (0.5297)	0.0837	0.806	1.223
0.580 (0.5800)	0.0837	0.833	1.100
0.610 (0.6100)	0.0830	0.846	1.027
0.650 (0.6500)	0.0835	0.862	0.929
0.672 (0.6720)	0.0803	?	0.874
0.680 (0.6800)	0.0829	0.861	...
0.701 (0.7008)	0.0808	0.829	...
0.731 (0.7307)	0.0803	0.787	...
1.000 (run 2)	0.0741
1.000 (run 3)	0.0694

$= (0.871 \pm 0.002)^\circ\text{K}$ and $x_0 = 0.6735 \pm 0.003$. These values may be compared to the values $T_0 = (0.872 \pm 0.003)^\circ\text{K}$ and $x_0 = 0.669 \pm 0.005$ suggested by the results of Graf, Lee, and Reppy.²

Within the three-phase region the data may be subjected to a self-consistency test of the following kind. In that region Eq. (5) implies that $c - (VT/N) \times (d^2P/dT^2)_\sigma$ is a linear function of x at fixed T . Likewise, Eq. (8) implies that in the same region the average liquid specific heat $c_{P,x}$ is a linear function of x , at fixed T . Although we have applied this test in both forms with similar results, we choose here to display it in the first form. Figure 4 shows plots for a series of temperatures with a "best" straight line drawn by eye through the points for each temperature. The linearity test is satisfied to within ± 0.02 J mole⁻¹ °K⁻¹ by much of the data. The points plotted in Fig. 4 are also listed in Table II.

The data for pure He³ were corrected in a manner like that used for the mixtures, and the results for $c_{P,x}$ were similarly tabulated and have been plotted in Fig. 5.²⁷ The good agreement between the two sets of results derived from separate runs with different sample sizes and thus different vapor-phase corrections is reassuring. The smooth curve in Fig. 5 represents the form suggested by Roberts, Sherman, and Sydoriak to represent earlier measurements of the specific heat c_{sat} ,¹⁷ corrected to yield $c_{P,x}$. The agreement between the curve and our data from 0.9 to 1.3 °K is extremely good. The tendency of our data outside of this temperature range to depart from the curve may reflect thermometer calibration problems towards both ends of the temperature scale that are not properly accounted for in Sec. III. Thus it is possible that errors in the mixture specific heats towards both ends of the scale are somewhat larger than estimated in that section.

We believe that the small bump in the specific heat of pure He³ at approximately 1.11 °K is spurious and arises from our failure to include the open-cell term $-(Tv/N)(dP/dT)(dN/dT)$ mentioned earlier in this section in obtaining $c_{P,x}$ from c . Although this term was negligibly small under most circumstances, it should have become large enough to have a noticeable effect at the point where the cell temperature reached the temperature of the He⁴ pot. At this point a rather rapid rise of the liquid level in the capillary should have taken place with increasing cell temperature.

V. ANALYSIS AND DISCUSSION

A. Three-Phase Region

The determinations of the quantity $c - (VT/N) \times (d^2P/dT^2)_\sigma$ given by the straight lines in Fig. 4 may be used in connection with Eq. (5) to determine $(d^2\mu_3/dT^2)_\sigma$ and $(d^2\mu_4/dT^2)_\sigma$ as unique functions of

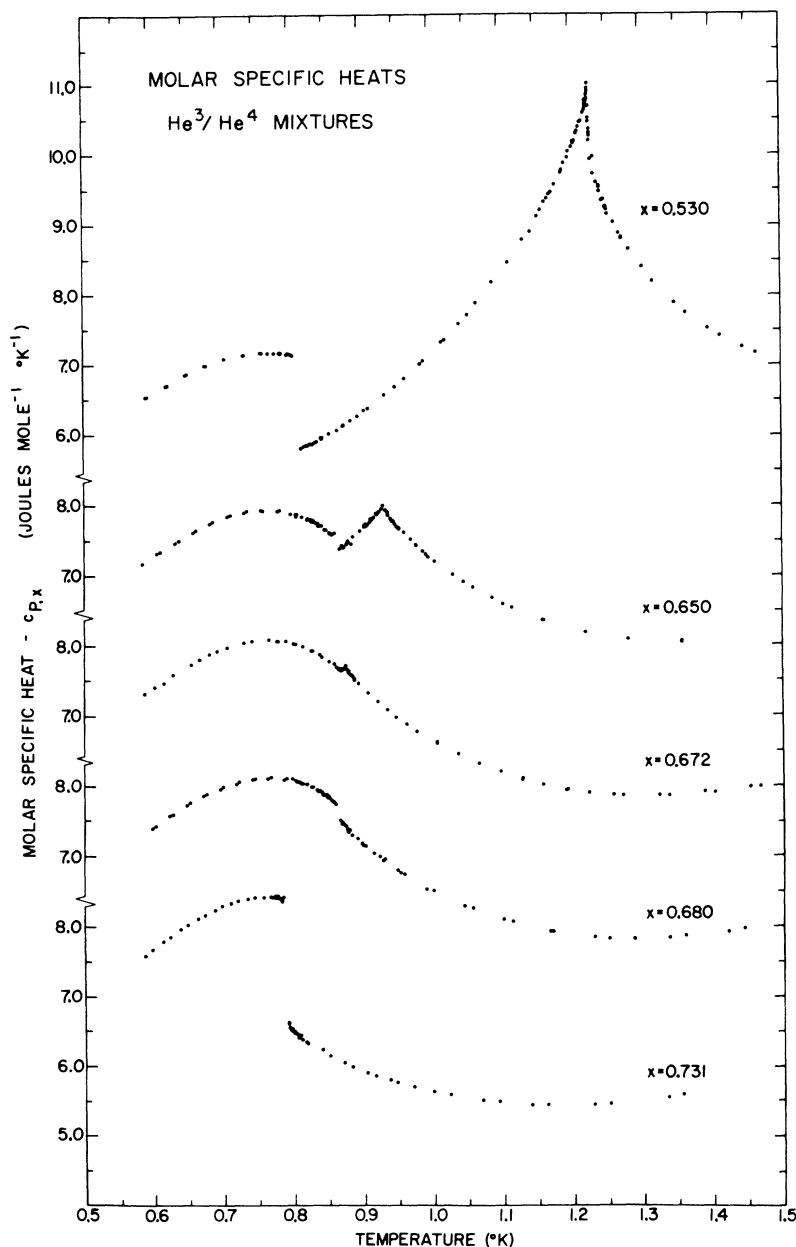


FIG. 2. Molar specific heat $c_{P,x}$ as a function of T for five representative values of x . Note the shifts in the vertical scale.

T in the three-phase region. However, because the extrapolations to $x=0$ and $x=1$ are long ones, we have chosen instead to determine the linearly related quantities $(d^2\phi/dT^2)_\sigma$ and $x_0(d^2\mu_3/dT^2)_\sigma + (1-x_0)(d^2\mu_4/dT^2)_\sigma$. At a given T the former is just $-1/T$ times the slope of the corresponding line in Fig. 4, while the latter is just $-1/T$ times the ordinate of the line at $x_0=0.6735$. The values of these quantities are listed in Table III and plotted as solid circles in Figs. 6 and 7.

Estimates of almost these same quantities may be made from the Leiden measurements of the specific heat of the mixtures in the two-liquid-phase

region,²⁸ and these estimates have been plotted as open circles in Figs. 6 and 7. It is also possible to estimate these quantities at temperatures ≤ 0.4 °K from other work. The derivative $(d^2\mu_4/dT^2)_\sigma$ in this region was obtained by twice differentiating along the He³-poor branch of the phase-separation curve the values of $\mu_4(x, T)$ calculated by Radebaugh for relatively small values of x .²⁹ The derivative $(d^2\mu_3/dT^2)_\sigma$ in this region was obtained from the measured specific heat of pure He³ as tabulated by Radebaugh²⁹ using the approximation that along the He³-rich branch of the phase-separation curve at low T the mixtures behave like regular solutions

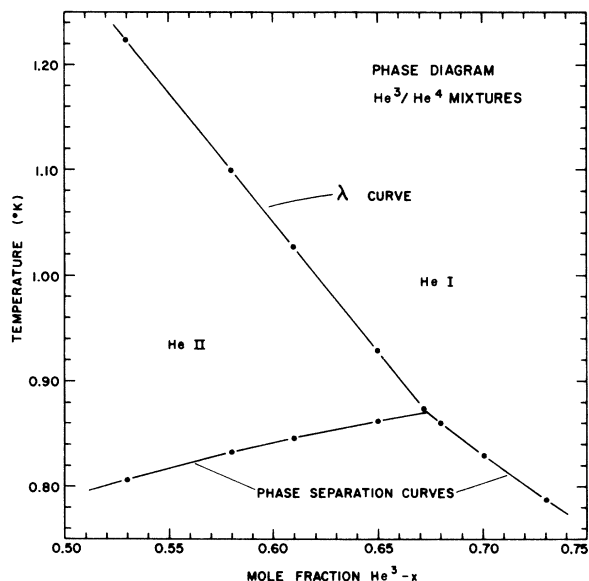


FIG. 3. Phase diagram for the mixtures near the junction as determined by our measurements of specific heat.

(simple mixtures). In so doing use was made of the regular-solution form for $\mu_3(x, T)$ used by Edwards and Daunt, together with their approximate form for the variation of x with T along the He³-rich branch of the phase-separation curve near $T = 0$.³⁰ Values of $(d^2\phi/dT^2)_\sigma$ and $x_0(d^2\mu_3/dT^2)_\sigma + (1-x_0)(d^2\mu_4/dT^2)_\sigma$ calculated from these estimates have been plotted as solid squares in Figs. 6 and 7.

With regard to $(d^2\phi/dT^2)_\sigma$, the values derived from our data do not agree well with the Leiden values in temperature dependence. However, a plausible interpolation may be made between our values and the values calculated for low temperatures, and the dashed line in Fig. 6 is simply

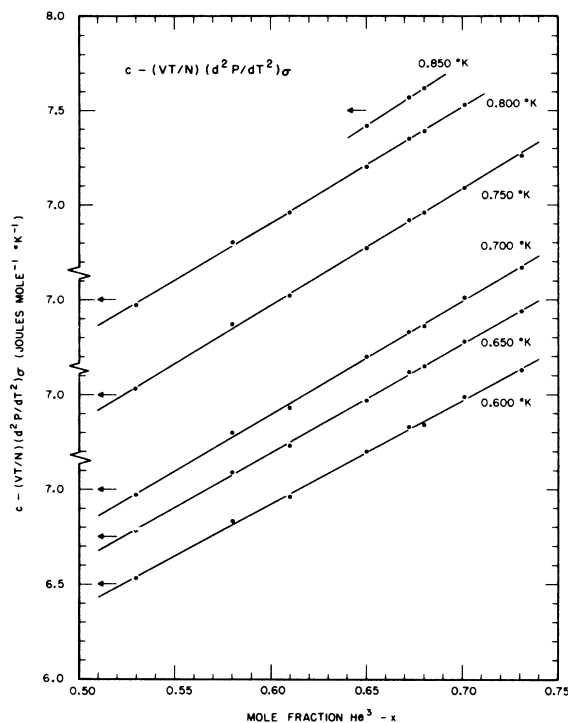


FIG. 4. Plots of $c - (VT/N)(d^2P/dT^2)_\sigma$ in the three-phase region as a function of x for six values of T . Note the shifts in the vertical scale; the arrow at the left-hand end of each line indicates the portion of the scale which applies to that line and to the points along it.

drawn by eye to provide this interpolation and to extrapolate our data to higher temperature.

With regard to $x_0(d^2\mu_3/dT^2)_\sigma + (1-x_0)(d^2\mu_4/dT^2)_\sigma$, the three sets of values connect with each other reasonably well, but the resulting function is not entirely convincing due to the differing temperature

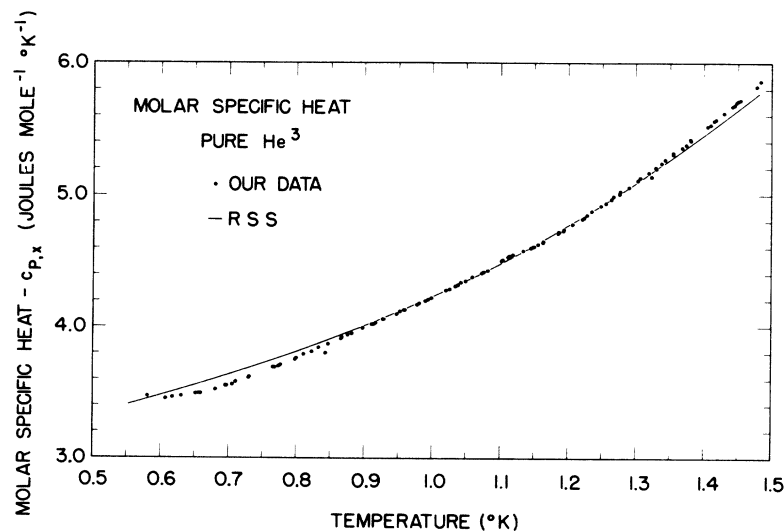
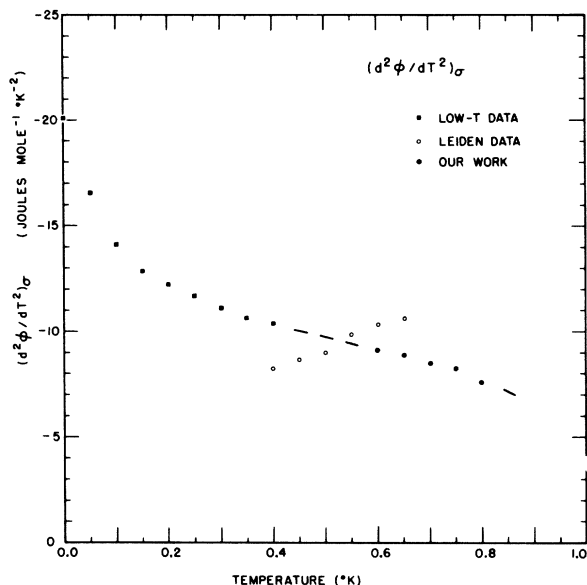
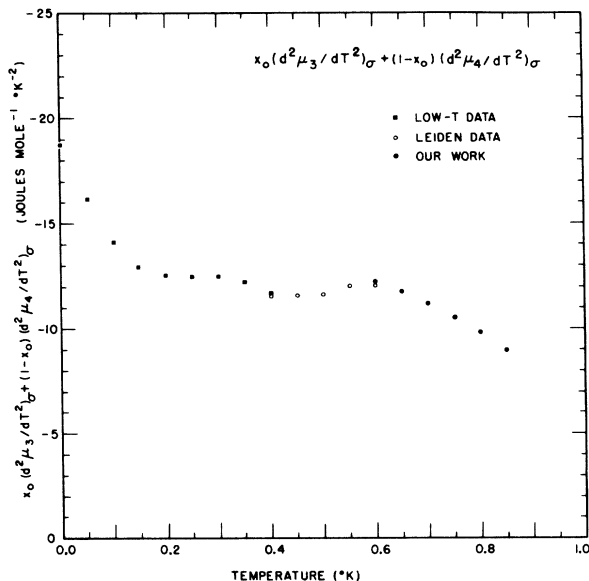


FIG. 5. Molar specific heat $c_{P,x}$ as a function of T for pure He³. The smooth curve was derived from the form for c_{sat} given by Roberts, Sherman, and Sydoriak (Ref. 17).

FIG. 6. Plot of $(d^2\phi/dT^2)_\sigma$ as a function of T .FIG. 7. Plot of $x_0(d^2\mu_3/dT^2)_\sigma + (1-x_0)(d^2\mu_4/dT^2)_\sigma$ as a function of T .

dependences. It seems clear that new specific-heat measurements at a number of values of x in the three-phase region from temperatures below 0.1 °K up to both branches of the phase-separation curve would be useful in determining more accurately the behavior of the mixtures in the three-phase region.

B. $(\partial\phi/\partial x)_{P,T}$ at Phase-Separation Curve

It can be seen from Eq. (8) that as a liquid mixture of average mole fraction x_l leaves the two-liquid-phase region and passes into the homogeneous phase at its phase-separation temperature T_σ , a discontinuity $\Delta c_{P,x}$ occurs in its average molar specific heat $c_{P,x}$ which is given by the expression

$$\Delta c_{P,x} = -T_\sigma \left(\frac{\partial\phi}{\partial x} \right)_{P,T} \left(\frac{dx}{dT} \right)_{P,\sigma}^2, \quad (9)$$

where $(\partial\phi/\partial x)_{P,T}$ applies to the homogeneous phase at x_l and T_σ , and $(dx/dT)_{P,\sigma}$ is the inverse slope of the phase-separation curve in the T, x plane at con-

stant pressure at the same point. Since for stability $(\partial\phi/\partial x)_{P,T}$ is always ≥ 0 , $\Delta c_{P,x}$ is always ≤ 0 .

Equation (9) provides a simple and direct way of determining $(\partial\phi/\partial x)_{P,T}$ for the liquid at the phase-separation curve, using the fact that $(dx/dT)_{P,\sigma}$ is believed to differ only negligibly from $(dx/dT)_\sigma$, the inverse slope of the phase-separation curve in the T, x plane at saturated vapor pressure. Values of $(\partial\phi/\partial x)_{P,T}$ at the phase-separation curve determined from our data are listed in Table IV along with the data from which they were calculated, and are plotted as solid circles in Fig. 8. The circles strongly suggest that $(\partial\phi/\partial x)_{P,T}$ goes to zero as the junction is approached along either branch of the phase-separation curve. The curves in Fig. 8 are merely smooth curves drawn by eye through the circles and through 0 at x_0 . Note the difference between the left and right vertical scales in Fig. 8 and thus the large asymmetry in $(\partial\phi/\partial x)_{P,T}$ at the phase-separation curve about x_0 .

TABLE II. The quantity $c - (VT/N)(d^2P/dT^2)_\sigma$ in the three-phase region as a function of T and x .

T (°K)	$c - (VT/N)(d^2P/dT^2)_\sigma$ (J mole ⁻¹ °K ⁻¹)							
x	0.530	0.580	0.610	0.650	0.672	0.680	0.701	0.731
0.600	6.53	6.83	6.96	7.20	7.33	7.34	7.49	7.63
0.650	6.78	7.09	7.23	7.47	7.62	7.65	7.78	7.94
0.700	6.97	7.30	7.43	7.70	7.83	7.86	8.01	8.17
0.750	7.03	7.37	7.52	7.77	7.92	7.96	8.09	8.26
0.800	6.97	7.30	7.46	7.70	7.85	7.89	8.03	...
0.850	7.42	7.57	7.62

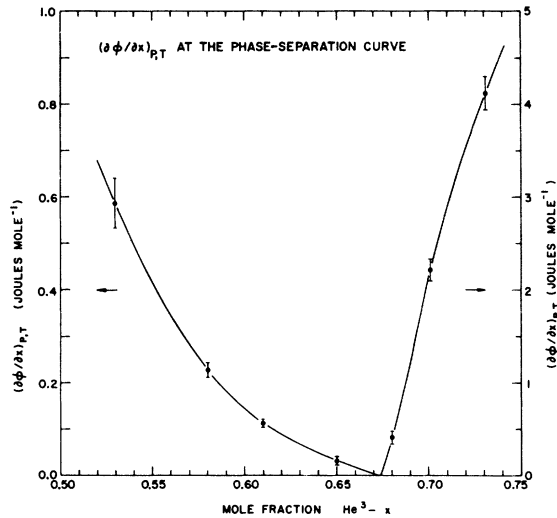


FIG. 8. Plot of $(\partial\phi/\partial x)_{P,T}$ at the phase-separation curve at saturated vapor pressure as a function of x . Note that different vertical scales have been used for the He^3 -rich and He^3 -poor branches.

The data shown in Fig. 8 further suggest that $(\partial\phi/\partial x)_{P,T}$ at the phase-separation curve goes to zero at the junction along either branch of the curve with finite nonzero slope as a function of x . As a result of the finite nonzero slopes of the two branches of the phase-separation curve in the T, x plane at the junction, a similar statement applies to plots of $(\partial\phi/\partial x)_{P,T}$ at the phase-separation curve as functions of temperature. In analogy with the conventional treatment of the liquid-vapor transition of an ordinary fluid in P, v, T space near its critical point, one may describe the asymptotic behavior of $(\partial\phi/\partial x)_{P,T}$ along either branch of the phase-separation curve by the expression

$$\left(\frac{\partial\phi}{\partial x}\right)_{P,T} \sim |T_0 - T|^{\gamma_{\pm}'} \quad (10)$$

where \pm refer to the He^3 -rich and He^3 -poor branches, respectively, and the γ_{\pm}' are two constants. Finite nonzero slopes for $(\partial\phi/\partial x)_{P,T}$ as

TABLE III. Values of $(d^2\phi/dT^2)_{\sigma}$ and $x_0(d^2\mu_3/dT^2)_{\sigma} + (1-x_0)(d^2\mu_4/dT^2)_{\sigma}$.

T (°K)	$\left(\frac{d^2\phi}{dT^2}\right)_{\sigma}$ (J mole ⁻¹ °K ⁻²)	$x_0\left(\frac{d^2\mu_3}{dT^2}\right)_{\sigma} + (1-x_0)\left(\frac{d^2\mu_4}{dT^2}\right)_{\sigma}$ (J mole ⁻¹ °K ⁻²)
0.600	-9.11	-12.21
0.650	-8.88	-11.72
0.700	-8.52	-11.20
0.750	-8.21	-10.56
0.800	-7.62	-9.82
0.850	...	-8.92

functions of T thus correspond to γ_{\pm}' both equal to unity. However, because of the lack of $(\partial\phi/\partial x)_{P,T}$ data close in to the junction and the uncertainties associated with the data points that do exist, it is essentially impossible to separate possibly non-analytic terms from whatever analytic background terms might be present and to determine γ_{\pm}' from such plots with any degree of certainty.

C. Thermodynamic Behavior near λ Line

In agreement with measurements of the specific heat of the liquid mixtures at lower values of x ,⁶ the λ anomaly in our measurements of $c_{P,x}$ decreases in height with increasing x and appears to become less singular. In particular, at x values near x_0 it appears that $c_{P,x}$ remains finite at $T_{\lambda}(x)$ and is continuous at that point. The derivative $(dc_{P,x}/dT)_x$ is evidently discontinuous at $T_{\lambda}(x)$, and although this derivative does not appear to diverge at $T_{\lambda}(x)$ for x near x_0 , differentiation of our data for $c_{P,x}$ at the lowest two values of x suggests that $(dc_{P,x}/dT)_x$ does indeed diverge, in agreement with the findings of Gasparini and Moldover at lower values of x .⁶

Our measurements with highest temperature resolution were made at $x=0.530$. The specific heat $c_{P,x}$ for this value of x near its λ temperature T_{λ} is shown in Fig. 9 as a function of $\ln|T - T_{\lambda}|$ for T both above and below T_{λ} .³¹ Although the tendency of these plots to level out as $\ln|T - T_{\lambda}| \rightarrow -\infty$ is clearly consistent with a finite limit for $c_{P,x}$ at T_{λ} , it would be dangerous to try to estimate this limit from the plot.³² The logarithm of the absolute value of the temperature derivative of these same data is shown versus $\ln|T - T_{\lambda}|$ in Fig. 10. In this figure the two curves for $T < T_{\lambda}$ represent two plausible alternative ways of treating the data in that region. The derivative $dc_{P,x}/dT$ appears to diverge as T_{λ} is approached from both above and below.

It is interesting to note that for values of x near x_0 the specific heat $c_{P,x}$ for the mixtures near T_{λ} bears a striking resemblance to the specific heat c_v for an ideal Bose gas near T_c .³³ The significance of this resemblance, if any, is not understood. We

TABLE IV. Quantities relating to the calculation of $(\partial\phi/\partial x)_{P,T}$ at the phase-separation curve.

x	$\Delta c_{P,x}$ (J mole ⁻¹ °K ⁻¹)	$(dT/dx)_{\sigma}$ (°K)	$(\partial\phi/\partial x)_{P,T}$ (J mole ⁻¹)
0.530	-1.34 ± 0.03	0.596 ± 0.026	0.589 ± 0.054
0.580	-0.84 ± 0.03	0.476 ± 0.014	0.229 ± 0.016
0.610	-0.54 ± 0.03	0.421 ± 0.011	0.113 ± 0.009
0.650	-0.18 ± 0.03	0.389 ± 0.032	0.032 ± 0.009
0.672
0.680	-0.16 ± 0.02	-1.480 ± 0.087	0.41 ± 0.07
0.701	-0.90 ± 0.03	-1.428 ± 0.031	2.22 ± 0.12
0.731	-1.69 ± 0.05	-1.390 ± 0.021	4.14 ± 0.18

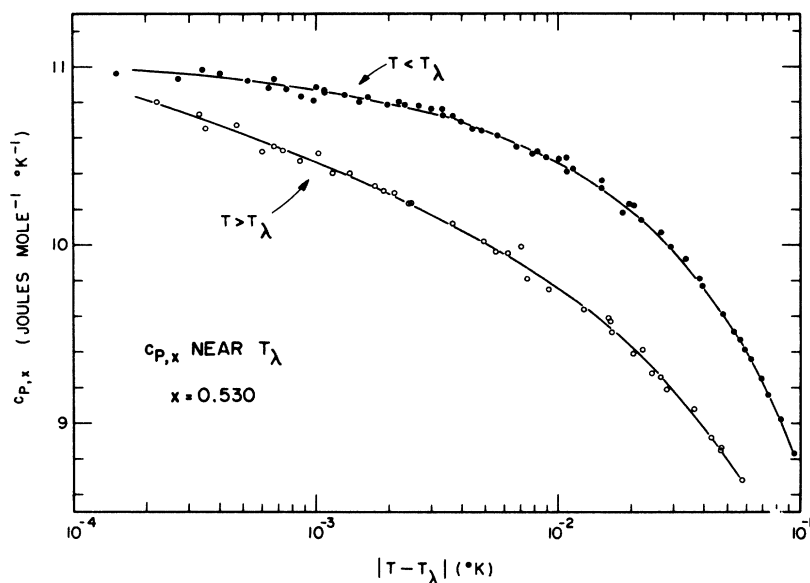


FIG. 9. Plots of $c_{P,x}$ for $x=0.530$ vs $\ln|T-T_{\lambda}|$ both above T_{λ} (open circles) and below T_{λ} (closed circles) (Ref. 31).

intend to publish a more complete analysis of our data in regard to behavior near the λ curve in a later paper.

D. Thermodynamic Behavior near Junction

The thermodynamic behavior of the mixtures observed near the junction differs in a number of ways from the "classical" behavior considered some years ago by Landau for the transformation of a second-order transition in a mixture into a first-order transition as the temperature is lowered through some critical temperature.³⁴ It followed from the assumptions made in the Landau model that discontinuities in the second partial derivatives

of the free energy occurred at the second-order transition and that the second-order transition curve and the "nonordered" branch of the phase-separation curve in T, x space (in our case, the He³-rich branch) met with equal slope.

In the mixtures, both the results of Graf, Lee, and Reppy² and our results give strong indications that the λ curve and He³-rich branch of the phase-separation curve meet with unequal slopes. Furthermore, $c_{P,x} = -T(\partial^2 g / \partial T^2)_{P,x}$ appears to be continuous across the λ curve. In addition, the vanishing of $(\partial \phi / \partial x)_{P,T}$ at the junction as the junction is approached from either side implies not only the continuity of $(\partial \phi / \partial x)_{P,T} = (\partial^2 g / \partial x^2)_{P,T}$ across the

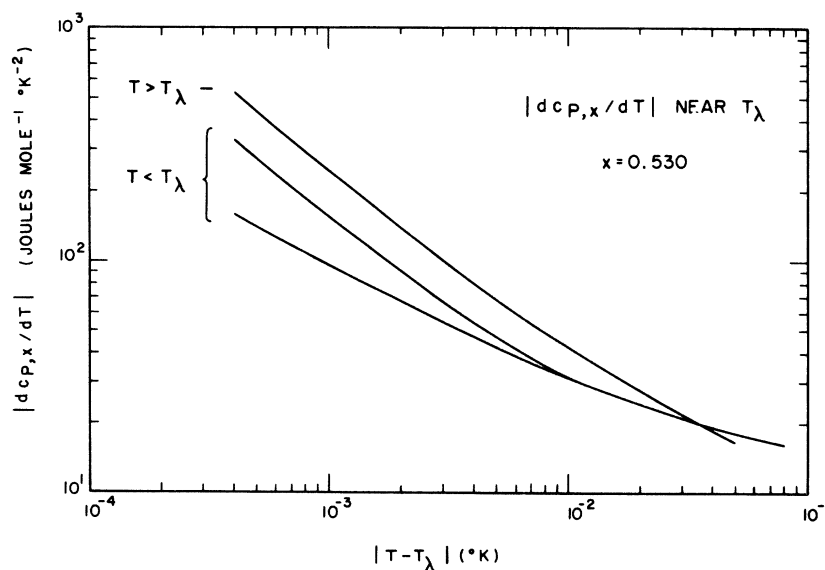


FIG. 10. Plots of $\ln|dc_{P,x}/dT|$ for $x=0.530$ vs $\ln|T-T_{\lambda}|$ both above and below T_{λ} . The two curves for $T < T_{\lambda}$ represent two plausible alternative ways of treating the data in that region.

λ curve at the junction but also the continuity of $(\partial\phi/\partial T)_{P,x} = (\partial^2 g/\partial x\partial T)_P$ at that point.

It may be noted in passing that as a result of the vanishing of $(\partial\phi/\partial x)_{P,T}$ at the junction we have the equalities

$$\left(\frac{d\phi}{dT}\right)_{P,\lambda;0} = \left(\frac{\partial\phi}{\partial T}\right)_{P,x;0} = \left(\frac{d\phi}{dT}\right)_{P,\sigma;0}, \quad (11)$$

where the subscript 0 is used to indicate derivatives evaluated at the junction. Hence in the T, ϕ plane at constant pressure, the phase-separation curve forms a smooth extension of the λ curve. However, $(d^2\phi/dT^2)_P$ along these curves may well be discontinuous at the junction.

Recently Griffiths has tentatively suggested a "nonclassical" scaling form for the free energy in the vicinity of the junction which is consistent with the distinctive features of the junction, namely, (a) nonzero slopes for the two branches of the phase-separation curve in T, x space at the point where they join the λ curve, both differing from that of the λ curve; (b) the vanishing of $(\partial\phi/\partial x)_{P,T}$ at the junction; (c) a continuous $c_{P,x}$ as a function of T at $x = x_0$; and (d) a continuous, finite, and cusped $c_{P,x}$ as a function of T at the λ curve for $x < x_0$.⁹ It is not yet clear, however, whether the Griffiths form can give an accurate representation of all of the thermodynamic behavior of the mixtures near the junction. We intend to present a more complete thermodynamic analysis of our data in the junction region in a later paper.

E. Gravitational Effects

Up to this point we have made no comment on the effect of gravity on our measurements near the λ curve and the junction of phase boundaries. For a mixture in a cell of finite height Δz in thermal equilibrium, gravity gives rise to both a vertical pressure gradient $dP/dz = -\rho g$ (where ρ is the mass density and g the gravitational acceleration) and a vertical ϕ gradient $d\phi/dz = (m_4 - m_3)g$ (where m_4 and m_3 are the molar masses of He⁴ and He³, respectively). These gradients will be accompanied by a vertical mole-fraction gradient dx/dz , and the net result will be a broadening and distortion of the critical features of $c_{P,x}$ as a function of T .

Calculation of the temperature scale on which such distortion should be apparent is made difficult by the lack of complete thermodynamic information about the mixtures in P, T, x (or P, T, ϕ) space. It is possible to separate the gravitational effect into the following two parts: The first is the effect due to the pressure gradient alone, supposing that no gradient in x were set up. The resultant broadening of the λ transition would be of the same type that is seen in measurements of c_P for pure He⁴ in a cell of finite height,³⁵ and since $(dT/dP)_{x,\lambda}$ is likely to be comparable to that for pure He⁴, the

broadening with our cell height of 3.0 cm is likely to have been several $\mu^\circ\text{K}$, considerably less than the resolution of our measurements.

However, the second part, due to the existence of a concentration gradient which becomes large as $(\partial\phi/\partial x)_{P,T}$ becomes small near the λ transition and the junction, appears to be the dominant effect. Rough estimates indicate that the broadening of the transition in our cell may well have been of the order of a few times 10^{-4}°K at $x = 0.530$ and a few times 10^{-3}°K at $x = 0.650$, just at the limits of our experimental resolution. The broadening at the junction may well have been even larger than this, and thus may possibly have had some influence on the critical features of the specific heat measured at $x = 0.672$. It is clear that it would be advantageous for this reason to use a sample of much smaller height in such measurements.

VI. ACKNOWLEDGMENTS

We are indebted to many people for their contributions to this work. In particular we would like to thank Miss M. Grönstrand and J. I. C. Ivarsson for help in taking and analyzing the data. We would also like to acknowledge the encouragement and support given this work by Professor O. V. Lounasmaa. One of us (W. Z.) is particularly indebted to Professor M. R. Moldover, Professor E. Byckling, and Dr. F. M. Gasparini for many helpful discussions of the work. He would also like to acknowledge the hospitality extended to him by the Department of Technical Physics of the Technical University of Helsinki and the support given him by a National Science Foundation Senior Postdoctoral Fellowship, a Fulbright Travel Grant, and the U. S. Atomic Energy Commission during different stages of the project.

APPENDIX: DERIVATION OF EQ. (6) FOR MOLAR SPECIFIC HEAT OF SAMPLE

We start with Eq. (5) in Sec. IV, which gives an expression for the over-all molar specific heat c of a sample consisting of N_3 moles of He³ and N_4 moles of He⁴ contained in a cell of fixed volume V :

$$c = -T \left(x \frac{d^2\mu_3}{dT^2} + (1-x) \frac{d^2\mu_4}{dT^2} \right) + \frac{VT}{N} \frac{d^2P}{dT^2}. \quad (\text{A1})$$

The notation used in this equation and in the following ones is explained in Sec. IV. It is convenient to rewrite this expression in the form

$$c = - \sum_i \frac{N_i}{N} T \left(x \frac{d^2\mu_3}{dT^2} + (1-x) \frac{d^2\mu_4}{dT^2} - v \frac{d^2P}{dT^2} \right)_i, \quad (\text{A2})$$

where i runs over whatever phases are present. Since μ_3 and μ_4 are uniform throughout the cell they can be evaluated in any of the phases present. However, for the i th term of the sum it is convenient to evaluate them in the i th phase. For $\mu_3(P, T, x)$

appropriate to the i th phase we have

$$\begin{aligned} \frac{d^2\mu_3}{dT^2} &= \left(\frac{\partial^2\mu_3}{\partial T^2}\right)_{P,x} + 2\left(\frac{\partial^2\mu_3}{\partial T\partial P}\right)_x \frac{dP}{dT} + 2\left(\frac{\partial^2\mu_3}{\partial T\partial x}\right)_P \frac{dx}{dT} \\ &+ \left(\frac{\partial^2\mu_3}{\partial P^2}\right)_{T,x} \left(\frac{dP}{dT}\right)^2 + 2\left(\frac{\partial^2\mu_3}{\partial P\partial x}\right)_T \frac{dP}{dT} \frac{dx}{dT} \\ &+ \left(\frac{\partial\mu_3}{\partial P}\right)_{T,x} \frac{d^2P}{dT^2} + \left(\frac{\partial^2\mu_3}{\partial x^2}\right)_{P,T} \left(\frac{dx}{dT}\right)^2 + \left(\frac{\partial\mu_3}{\partial x}\right)_{P,T} \frac{d^2x}{dT^2}, \end{aligned} \quad (A3)$$

where the subscript i has been omitted for simplicity.

A similar expression holds for $d^2\mu_4/dT^2$. Now we may insert these expressions for $d^2\mu_3/dT^2$ and $d^2\mu_4/dT^2$ into Eq. (A2), simplifying the resulting expression by use of a number of relations between partial derivatives derived from the Gibbs-Duhem relation:

$$x_i d\mu_3 + (1-x_i) d\mu_4 = -s_i dT + v_i dP. \quad (A4)$$

The relationships which result are as follows:

$$x \left(\frac{\partial\mu_3}{\partial P}\right)_{T,x} + (1-x) \left(\frac{\partial\mu_4}{\partial P}\right)_{T,x} = v, \quad (A5)$$

$$x \left(\frac{\partial\mu_3}{\partial T}\right)_{P,x} + (1-x) \left(\frac{\partial\mu_4}{\partial T}\right)_{P,x} = -s, \quad (A6)$$

$$x \left(\frac{\partial\mu_3}{\partial x}\right)_{P,T} + (1-x) \left(\frac{\partial\mu_4}{\partial x}\right)_{P,T} = 0, \quad (A7)$$

$$x \left(\frac{\partial^2\mu_3}{\partial P^2}\right)_{T,x} + (1-x) \left(\frac{\partial^2\mu_4}{\partial P^2}\right)_{T,x} = \left(\frac{\partial v}{\partial P}\right)_{T,x}, \quad (A8)$$

$$x \left(\frac{\partial^2\mu_3}{\partial T^2}\right)_{P,x} + (1-x) \left(\frac{\partial^2\mu_4}{\partial T^2}\right)_{P,x} = -\left(\frac{\partial s}{\partial T}\right)_{P,x}, \quad (A9)$$

$$x \left(\frac{\partial^2\mu_3}{\partial x^2}\right)_{P,T} + (1-x) \left(\frac{\partial^2\mu_4}{\partial x^2}\right)_{P,T} = -\left(\frac{\partial\phi}{\partial x}\right)_{P,T}, \quad (A10)$$

$$x \left(\frac{\partial^2\mu_3}{\partial P\partial T}\right)_x + (1-x) \left(\frac{\partial^2\mu_4}{\partial P\partial T}\right)_x = \left(\frac{\partial v}{\partial T}\right)_{P,x} = -\left(\frac{\partial s}{\partial P}\right)_{T,x}, \quad (A11)$$

$$x \left(\frac{\partial^2\mu_3}{\partial T\partial x}\right)_P + (1-x) \left(\frac{\partial^2\mu_4}{\partial T\partial x}\right)_P = 0, \quad (A12)$$

$$x \left(\frac{\partial^2\mu_3}{\partial x\partial P}\right)_T + (1-x) \left(\frac{\partial^2\mu_4}{\partial x\partial P}\right)_T = 0, \quad (A13)$$

where again the subscript i has been omitted for simplicity.

As a result we obtain the desired expression

$$c = \sum_i \frac{N_i}{N} \left[c_{P,x} - 2T \left(\frac{\partial v}{\partial T}\right)_{P,x} \frac{dP}{dT} - T \left(\frac{\partial v}{\partial P}\right)_{T,x} \left(\frac{dP}{dT}\right)^2 + T \left(\frac{\partial\phi}{\partial x}\right)_{P,T} \left(\frac{dx}{dT}\right)^2 \right]_i. \quad (A14)$$

As the sample is heated, not only are the individual phases warmed but in addition there is transfer of material from one phase to another. Although the expression above takes the form of a sum over the individual phases, it does in fact include contributions from both effects. In the special case of a one-component system ($x=0$, say) the expression given above may be compared to that given by Hill and Lounasmaa.³⁶ Although the two expressions are somewhat different in form, in particular the one derived here containing no terms proportional to d^2P/dT^2 , they are, in fact, equivalent. The absence of the d^2P/dT^2 term may in some situations make the present expression more convenient than that of Hill and Lounasmaa.

*Work supported in part by the U. S. Atomic Energy Commission under Contract No. AT(11-1)-1569. This report is designated C00-1569-79.

†Present address: Department of Physics, University of Lancaster, Lancaster, United Kingdom.

¹For a general review of work on the mixtures prior to 1964 see K. W. Taconis and R. de Bruyn Ouboter, in *Progress in Low Temperature Physics*, edited by C. J. Gorter (North-Holland, Amsterdam, 1964), Vol. IV, Chap. 2.

²E. H. Graf, D. M. Lee, and J. D. Reppy, *Phys. Rev. Letters* **19**, 417 (1967).

³O. K. Rice, *Phys. Rev. Letters* **19**, 295 (1967).

⁴R. de Bruyn Ouboter, K. W. Taconis, C. le Pair, and J. J. M. Beenakker, *Physica* **26**, 853 (1960).

⁵T. Alvesalo, P. Berglund, S. Islander, G. R. Pickett, and W. Zimmermann, Jr., *Phys. Rev. Letters* **22**, 1281 (1969).

⁶F. Gasparini and M. R. Moldover, *Phys. Rev. Letters* **23**, 749 (1969); F. M. Gasparini, Ph.D. thesis (University of Minnesota, 1970) (unpublished).

⁷T.-H. Tang, C. Zipfel, and E. H. Graf, *Bull. Am.*

Phys. Soc. **15**, 530 (1970).

⁸G. Goellner and H. Meyer, *Phys. Rev. Letters* **26**, 1534 (1971).

⁹R. B. Griffiths, *Phys. Rev. Letters* **24**, 715 (1970).

¹⁰R. B. Griffiths and J. C. Wheeler, *Phys. Rev. A* **2**, 1047 (1970).

¹¹E. C. Kerr, *Phys. Rev. Letters* **12**, 185 (1964); and private communication.

¹²Models No CG-4 (Thermometer A) and CG-1 (Thermometer B), Radiation Research Corp. (Andonian Associates, Inc., Waltham, Mass.).

¹³R. W. Hill and G. R. Pickett, *Ann. Acad. Sci. Fenn. Ser. A VI* **210**, 40 (1966).

¹⁴T. P. Ptukha, *Zh. Eksperim. i Teor. Fiz.* **39**, 896 (1960) [*Sov. Phys. JETP* **12**, 621 (1961)].

¹⁵R. H. Sherman, S. G. Sydorik, and T. R. Roberts, *J. Res. Natl. Bur. Std. (U.S.)* **68A**, 579 (1964).

¹⁶A. C. Anderson, *Cryogenics* **8**, 50 (1968).

¹⁷T. R. Roberts, R. H. Sherman, and S. G. Sydorik, *J. Res. Natl. Bur. Std. (U.S.)* **68A**, 567 (1964).

¹⁸T. R. Roberts and S. G. Sydorik, *Phys. Rev.* **102**, 304 (1956).

¹⁹Model No. 144 with capsule type 1, Texas Instruments, Inc., Houston, Tex.

²⁰W. H. Keesom, *Helium* (Elsevier, Amsterdam, 1942).

²¹R. E. Barieau, *J. Phys. Chem.* **72**, 4079 (1968).

²²S. G. Sydoriak and T. R. Roberts, *Phys. Rev.* **118**, 901 (1960).

²³T. R. Roberts and B. K. Swartz, in *Proceedings of the Second Symposium on Liquid and Solid Helium Three*, edited by J. G. Daunt (Ohio State U. P., Columbus, Ohio 1960).

²⁴R. de Bruyn Ouboter, J. J. M. Beenakker, and K. W. Taconis, *Physica* **25**, 1162 (1959).

²⁵T. R. Roberts and S. G. Sydoriak, *Phys. Fluids* **3**, 895 (1960).

²⁶M. J. Buckingham and W. M. Fairbank, in *Progress in Low Temperature Physics*, edited by C. J. Gorter (North-Holland, Amsterdam, 1961), Vol. III, Chap. 3.

²⁷Complete tables of the values of $c_{P,x}$ so determined may be obtained from the last author (W. Z.).

²⁸Reference 4, Fig. 12. Note that these measurements were made with a full cell and at a pressure that was

probably somewhat above saturated vapor pressure. Therefore, the specific heat measured was not strictly the same as our c , although the difference is likely to have been quite small.

²⁹R. Radebaugh, Nat. Bur. Std. (U.S.) Technical Note No. 362, 1967 (unpublished).

³⁰D. O. Edwards and J. G. Daunt, *Phys. Rev.* **124**, 640 (1961).

³¹In making the plots of Fig. 9 from the tabulated data for $c_{P,x}$, shifts in T_λ of up to 1.0 m°K between the separate series of points involved were allowed in order to bring the data of these series into better agreement.

³²M. E. Fisher and P. E. Scesney, *Phys. Rev. A* **2**, 825 (1970).

³³F. London, *Superfluids* (Wiley, New York, 1954), Vol. II, Sec. 7.

³⁴*Collected Papers of L. D. Landau*, edited by D. ter Haar (Pergamon Press, Oxford, 1965), p. 193.

³⁵G. Ahlers, *Phys. Rev.* **171**, 275 (1968).

³⁶R. W. Hill and O. V. Lounasmaa, *Phil Mag.* **2**, 143 (1957).

PHYSICAL REVIEW A

VOLUME 4, NUMBER 6

DECEMBER 1971

Validity of the Quasisteady State and Collisional-Radiative Recombination for Helium Plasmas. I. Pure Afterglows*

C. C. Limbaugh†

Arnold Engineering Development Center, Arnold Air Force Station, Tennessee

and

A. A. Mason‡

The University of Tennessee Space Institute, Tullahoma, Tennessee

(Received 6 February 1971)

The set of differential equations describing the time-dependent decay of a singly ionized optically thin monatomic gas has been solved numerically for constant-temperature-constant-pressure helium afterglows. In the range of conditions studied ($6000 \leq T_e \leq 14\,000$ °K, $1.5 \times 10^{12} \leq n_e \leq 5.38 \times 10^{15}$ cm⁻³, $1.5 \times 10^{14} \leq n_0 \leq 1.63 \times 10^{17}$ cm⁻³) it was found that collisional-radiative recombination can be applied to the electron-density decay before the plasma reaches the quasisteady state. The initial condition for each plasma studied was a Boltzmann distribution from the 2^3S state throughout the higher states. The mechanism by which the quasisteady state is obtained is examined and the transient coupling between states is illustrated. Times for the plasma to reach the quasisteady state ranged from $t \approx 10^{-8}$ sec for high-density plasmas to $t \approx 10^{-4}$ sec for low-density plasmas.

I. INTRODUCTION

The study of recombining plasmas was considerably enhanced by the development of the collisional-radiative recombination (CRR) theory by Bates, Kingston, and McWhirter¹ for hydrogenic plasmas. Their work included three-body recombination² along with the other salient processes contributing to plasma decay to obtain effective collisional-radiative recombination and collisional-radiative ionization coefficients which describe the plasma decay. In order to obtain their results, however, it is necessary to impose the quasisteady state

(QSS) assumption in which all quantum levels, with the exception of the ground state, do not suffer a temporal change in population density. Another approach^{3,4} to obtaining CRR coefficients utilizing the fact that there is a minimum in the total rate of deexcitation of atoms as a function of the energy levels has been used but this also requires the QSS assumption.

The results of CRR theory and the QSS assumption have been used by many investigators (e.g., Refs. 5–8) to interpret results for helium plasmas with varying degrees of success. Although in much of the work the existence of the molecular